published in *Science* **295**, 1691 (2002)

Quantum Impurities in the Two-Dimensional Spin One-Half Heisenberg Antiferromagnet

O.P. Vajk[1], P.K. Mang[2], M. Greven[2,3*], P.M. Gehring[4], J.W. Lynn[4]

[1] Department of Physics, Stanford University, Stanford, CA 94305, USA.

[2] Department of Applied Physics, Stanford University, Stanford, CA 94305, USA.

[3] Stanford Synchrotron Radiation Laboratory, Stanford, CA 94309, USA.

[4] NIST Center for Neutron Research, National Institute of Standards and Technology, Gaithersburg, MD 20899, USA.

*To whom correspondence should be addressed; E-mail: greven@stanford.edu.

The study of randomness in low-dimensional quantum antiferromagnets is at the forefront of research in the field of strongly correlated electron systems, yet there have been relatively few experimental model systems. Complementary neutron scattering and numerical experiments demonstrate that the spin-diluted Heisenberg antiferromagnet $La_2Cu_{1-z}(Zn,Mg)_zO_4$ is an excellent model material for square-lattice site percolation in the extreme quantum limit of spin one-half. Measurements of the ordered moment and spin correlations provide important quantitative information for tests of theories for this complex quantum-impurity problem.

The field of low-dimensional quantum magnetism has been of enormous interest to the condensed-matter physics community ever since the discovery that La_2CuO_4, the parent compound of the original high-temperature superconductor $(La,Ba)_2CuO_4$, is a model two-dimensional (2D) quantum (spin-1/2) antiferromagnet. Because the superconductivity occurs in the vicinity of an antiferromagnetic phase in these materials, it appears likely that antiferromagnetic fluctuations are at least partially responsible for their rich physics. One of the new frontiers in condensed-matter physics lies in the field of quantum critical behavior, especially of "dirty" low-dimensional systems involving quantum impurities [1]. Although there has been much progress in the experimental investigation of quantum impurities in the simpler 1D $S = 1/2$ chain [2] and ladder compounds [3], experiments with the 2D analog have been restricted to low impurity concentrations because of the lack of suitable samples [4, 5, 6, 7].

We have investigated the properties of the spin-1/2 square-lattice Heisenberg antiferromagnet (SLHAF) in the presence of a significant density z of quenched, spinless quantum impurities, up to and through the percolation threshold. Specifically, the combined experimental and numerical results for the ordered moment $M_{st}(z)$ and spin correlations $\xi(z,T)$ demonstrate that $La_2Cu_{1-z}(Zn,Mg)_zO_4$ is well described by the Hamiltonian

$$\mathcal{H} = \quad J \quad \sum_{\langle i,j \rangle} p_i p_j \mathbf{S}_i \cdot \mathbf{S}_j, \tag{1}$$

where the sum is over nearest-neighbor (NN) sites, J is the antiferromagnetic Cu-O-Cu superexchange, $\mathbf{S}_i$ is the $S = 1/2$ operator at site i, $p_i = 1$ on magnetic sites, and $p_i = 0$ on non-magnetic sites.

In the absence of quantum fluctuations, the NN square lattice undergoes a geometric transition with site dilution z at the percolation threshold $z_p \approx 40.725\%$ [8, 9]. As indicated in Fig. 1, below this concentration there is always one cluster of connected sites that spans the infinite lattice. Above z_p, the lattice consists entirely of finite-sized clusters. In studies of site-diluted $S = 5/2$ Heisenberg and Ising antiferromagnets, long-range order was found to disappear only above z_p [10]. However, in the extreme quantum limit of $S = 1/2$, previous measurements of the Néel temperature T_N extrapolated to $T_N = 0$ well below z_p [4, 5, 6], and the possible existence of a new quantum critical point at $z_{S=1/2} < z_p$ has also been raised based on theoretical [11, 12] and numerical [13] considerations. Recent Monte Carlo simulations of Eq. 1 suggest that the site-diluted $S = 1/2$ SLHAF remains ordered up to the percolation threshold [14, 15], but possibly with new, non-classical critical exponents [14]. Our experimental data allow us to rule out the existence of a quantum critical point significantly below z_p, and we find that $M_{st}(z)$ is reasonably well described, up to $z \approx 30\%$, by a recent combined spin-wave theory and T-matrix approach [16].

In addition to information about the ground state properties, knowledge of the temperature and doping dependence of the 2D instantaneous spin-spin correlation length, $\xi(z,T)$, provides valuable information about the dynamics of the spin degrees of freedom. Neutron scattering studies of the spin correlations of La_2CuO_4 [17] and related materials [18, 19], as well as numerical results [20], have served as important tests of theories for Eq. 1 in the absence of quantum impurities [21, 22]. Remarkably, even though the quenched disorder leads to the loss of Lorentz invariance, a quantum non-linear sigma model approach developed for Eq. 1 in the absence of disorder is found to give an excellent effective description of $\xi(z,T)$ up to at least $z = 35\%$. Our experimental and numerical results can help guide the development of an underlying theory for the randomly diluted system.

Several experimental difficulties have previously prevented quantitative experimental studies of randomly diluted La_2CuO_4. First, the highest reported concentration of non-magnetic

ions is 25% [4], still well below z_p. Second, single crystal results have been limited even further, to $z \approx 15\%$ [5, 7]. Third, the excess oxygen typically found in as-grown samples introduces holes into the copper-oxygen sheets, which frustrate the antiferromagnetism and quickly destroy magnetic order [23]. Differing values for $T_N(z)$ indicate that this problem has not been fully resolved [4, 5, 6, 7].

By jointly substituting Zn and Mg on the Cu site, we were able to grow $La_2Cu_{1-z}(Zn,Mg)_zO_{4+\delta}$ crystals by the traveling-solvent floating-zone method. The Zn content was approximately 10% whereas the Mg content varied. Typical single grain sections were 40 mm long and 4 mm in diameter. Both Zn^{2+} and Mg^{2+} are non-magnetic, effectively removing a magnetic site without introducing charge carriers. Zn^{2+} has a larger ionic radius than Cu^{2+}, and Mg^{2+} has a smaller ionic radius than Cu^{2+}. Compositional analysis was carried out by electron probe microanalysis on end sections of the crystals. The samples were carefully reduced at $T = 900$ to 950 °C in Ar flow. Several crystals used for neutron scattering had a small Cu/Zn/Mg concentration gradient, typically 1 to 2% dilution, along the full length of the crystal. Mosaic widths were very good, 15' full width at half maximum (FWHM) or less. Small, very homogeneous sections a few cubic millimeters in size were cut from the larger crystals for magnetometry. Polycrystalline samples, with concentrations assumed to be equal to their nominal values, yielded similar magnetometry results.

Elastic scattering at the $(1, 0, 0)$ Bragg peak (orthorhombic notation), shown in Fig. 2A, was used to determine T_N and $M_{st}(z)$. We find long-range Néel order even at $z = 39\%$, where T_N is only 8 K. Figure 2B shows our result for $T_N(z)$. Below $z \approx 20\%$, the data agree well with the linear behavior found in previous experimental [4, 5, 6] and recent theoretical [16] work. However, we find that T_N falls off more gradually at higher concentrations. Quantum fluctuations for $S = 1/2$ apparently are not strong enough to noticeably shift the critical point: $z_{S=1/2} = z_p$, within the uncertainty of our experiment.

In order to probe the ground state properties of $La_2Cu_{1-z}(Zn,Mg)_zO_4$ we have extracted $M_{st}(z)$ from the low-temperature (1,0,0) intensity. To facilitate normalization between samples, we measured the intensity of a standard phonon for each sample to determine the illuminated volume; normalizing by sample mass gives the same result within the errors. The resulting normalized moment per Cu atom is plotted in Fig. 2C. Our data are consistent with previous nuclear quadrupole resonance(NQR) measurements below $z = 15\%$ [6]. Numerical results for Eq. 1 deviate somewhat in their magnitude, but also suggest that $z_{S=1/2} = z_p$ [14, 15]. Recent theory [16], which uses a spin-wave theory and T-matrix approach and is expected to be valid at low and intermediate concentrations, gives a good description of our data up to $z \approx 30\%$. The classical ($S \to \infty$) behavior is significantly different, because the reduction of the moment is attributed only to Cu sites being disconnected from the infinite cluster. It should be noted that already $M_{st}(0)$ is reduced from the classical value $M_{st,cl}(0) = 1/2$ by about 40% because of quantum fluctuations [20, 24]. These fluctuations evidently increase with dilution, further weakening the ordered moment, but not sufficiently to disorder the system below z_p. The experimental data are well described by a power law with $z_{S=1/2} = z_p$ and an effective exponent $\beta_{eff} = 0.45(3)$. In their finite-size scaling analysis, Kato et al. [14] extracted spin-dependent critical exponents, with $\beta = 0.46$ for $S = 1/2$, which is substantially different from the classical value $\beta_{cl} = 5/36$ [8]. However, it has been argued that these are not the true critical exponents, which should equal the classical values [15].

We also performed a systematic study of the instantaneous 2D spin-spin correlation length $\xi(z, T)$ in the paramagnetic phase of $La_2Cu_{1-z}(Zn,Mg)_zO_4$. The equal-time structure factor was measured in two-axis, energy-integrating mode [17]. Figure 3A shows representative data for $z = 19\%$ at $T = 200$ K. The scattering broadens as ξ decreases, both with increasing temperature and increasing dilution. Correlation lengths were obtained from fits to a Lorentzian,

$\sim 1/(1+q_{2D}^2\xi^2)$, where q_{2D} is the 2D momentum transfer component in the CuO_2 sheets relative to the zone center at $H = 1$, convoluted with the instrumental resolution. The extracted lengths are plotted versus J/T in Fig. 3B. The data shown were cut off above T_N by 1 SD (≈ 4 K), as obtained from fits of the order parameter assuming a Gaussian distribution in T_N (Fig. 2A). Temperature is scaled by $J = 135$ meV, the antiferromagnetic superexchange energy of the pure system [17]. The data reveal that doping significantly decreases the rate at which correlations grow as the system is cooled. Specifically, at high concentrations $\xi(z,T)$ crosses over from exponential to power-law behavior. We note that the $z = 40(2)$% and 43(2)% samples do not exhibit Néel order at 1.4 K ($J/T \approx 1100$), and the spin correlations appear to approach a constant zero-temperature value, as expected for $z > z_p$.

In order to test the degree to which the experimental system is described by Eq. 1, we have performed quantum Monte Carlo (QMC) simulations to calculate $\xi(z,T)$. We used the loop-cluster algorithm, which is suited to study the randomly diluted Heisenberg model [25]. Lattice sizes 10 to 20 times larger than the correlation length were used in order to avoid finite-size effects. We were able to perform our calculations on very large lattices of up to 1700×1700 sites and to temperatures as low as $T = J/100$. Previous numerical work involved system sizes as large as 20×20 [13, 26] and reached $T = J/2$ [26] and $T = J/20$ [13]. Between 5 and 200 configurations were averaged for each temperature and concentration, and we chose 10^4 to 10^5 equilibrations and 10^4 to 10^5 measurements per configuration. The QMC results (Fig. 3B) extend to higher temperatures and thus complement the experiment, covering a combined three orders of magnitude in temperature. We emphasize that this comparison contains no adjustable parameters, because J is known rather well for the experimental system. We find excellent quantitative agreement up to the percolation threshold.

The ground state of the pure SLHAF is ordered, but quantum fluctuations renormalize the spin-wave velocity, $c = 2\sqrt{2}SZ_cJa$, and spin-stiffness, $\rho_s = S^2Z_\rho J$, from their classical values (we use units in which $g\mu_B = k_B = \hbar = 1$). For $S = 1/2$ and $z = 0$, the quantum renormalization factors Z_c and Z_ρ are known from various theoretical and numerical studies. Using these quantities, $\xi(z = 0,T)$ is quantitatively given by [21, 22]

$$\frac{\xi}{a} = \frac{e}{8}\frac{c/a}{2\pi\rho_s}e^{2\pi\rho_s/T}\left[1 - \frac{1}{2}\left(\frac{T}{2\pi\rho_s}\right) + \mathcal{O}\left(\frac{T}{2\pi\rho_s}\right)^2\right]. \tag{2}$$

Even though Eq. 2 is strictly valid only at asymptotically low temperatures [20, 21, 22], it agrees remarkably well with experiment [17, 18, 19] and numerics [20] for $S = 1/2$ in the range $2 < \xi/a < 200$ shown in Fig. 3B. The derivation of Eq. 2 involves a mapping of the discrete Heisenberg Hamiltonian Eq. 1 to a quantum non-linear sigma model (QNLσM), and it is based on the assumptions of an ordered ground state and of translational invariance. Random dilution breaks translational invariance of the SLHAF and leads to defect rods in the time-like direction of the effective QNLσM. The latter implies the loss of Lorentz invariance, and a QNLσM description may no longer remain valid [21, 16]. Nevertheless, it is valuable to test the extent to which this description may hold. Because there exist no accurate predictions for $c(z)$ and $\rho_s(z)$, such a test requires us to treat these zero-temperature quantities as fit parameters. A modified form of Eq. 2,

$$\frac{\xi}{a} = \frac{e}{8}\frac{c/a}{2\pi\rho_s}\frac{e^{2\pi\rho_s/T}}{1 + (4\pi\rho_s/T)^{-\nu_T}} \tag{3}$$

with $\nu_T = 1$, has been suggested for disorder-free systems approaching a quantum critical point [27], where $\rho_s = 0$ and $\xi \sim 1/T$ [21]. Even though $z_{S=1/2} = z_p$ may not be a quantum

critical point, random dilution reduces the spin stiffness and may be viewed as bringing the system closer to such a point in an extended parameter space. In a classical picture, $z = z_p$ is a (geometric and thermal) multi-critical point, and $\rho_s = 0$ as well as power-law behavior are expected. The thermal correlation length exponent $\nu_T = 0.90(5)$ was previously determined for the $S = 5/2$ system $Rb_2(Mn,Mg)F_4$ [10]. Furthermore, for $z > z_p$ it was found that the data were well described by the form

$$\frac{1}{\xi(z,T)} = \frac{1}{\xi_0(z)} + \frac{1}{\xi_T(T)} \tag{4}$$

where ξ_0 is a zero-temperature length, possibly reduced from the geometric length of the percolation problem by small quantum fluctuations, and $\xi_T \sim T^{-\nu_T}$.

We find that Eq. 2 gives a very good description of our data, especially at lower concentrations, and for $\xi/a > 8$ to 10 at $z = 31\%$ and 35%. The modified form Eq. 3, however, even captures the high-temperature power-law behavior at the higher concentrations. Results of fits to Eq. 3 of our QMC data for $z < z_p$ are shown in Fig. 3B and summarized in Table I. Fits to Eq. 2 result in large uncertainties in the value of the spin-wave velocity, but $\rho_s(z)$ and $c(z)$ extracted using these two forms agree within the errors. For the pure system, a fit of numerical data [20] below $\xi/a = 200$ yields $2\pi\rho_s(0) = 1.18(1)J$ and $c(0) = 1.33(3)Ja$, about 4% higher and 20% lower, respectively, than the most accurate estimate [20]. A recent combined QNLσM, and percolation theory approach [12] resulted in

$$\frac{\rho_s(z)}{\rho_s(0)} = A(z)\left[1 - \frac{\bar{g}(0)}{P_\infty(z)}\right]\frac{1}{1-\bar{g}(0)}, \tag{5}$$

where $\bar{g}(0) = 0.685$ is the coupling constant corresponding to the $S = 1/2$ SLHAF at $z = 0$ [21], and $A(z)$ and $P_\infty(z)$ are the bond dilution factor and the probability of finding a spin in the infinite cluster. The latter two quantities are well described up to $z \approx 37\%$ and $z \approx 30\%$, respectively, by $A(z) \approx 1 - \pi z + \pi z^2/2$ and $P_\infty(z) \approx 1 - z$ [8, 28]. Equation 5 incorrectly predicts $\rho_s(z \approx 30\%) = 0$, and hence a quantum critical point well below the percolation threshold [12]. To our surprise, we find that substituting $1 + z$ for $1/P_\infty(z)$ *quantitatively* describes $\rho_s(z)/\rho(0)$ even at $z = 35\%$, as shown in Table 1. This substitution is correct at low concentrations and prevents the second term in Eq. 5 from going to zero below z_p. We note that Eq. 5 is a one-loop renormalization-group result, and higher-order terms can be expected to improve agreement with our observations. The expression for the spin-wave velocity that corresponds to Eq. 5 [12], $c(z)/c(0) = A(z)(1 + z/2)$, decreases monotonically with dilution, and hence does not describe the behavior found from our fits (see Table 1).

For $z > z_p$, the joint experimental ($z = 40(2)\%$ and $z = 43(2)\%$) and numerical ($z = 41\%$ and $z = 46\%$) data are fit to Eq. 4. Better results are obtained if $1/\xi_0$ is allowed to be non-zero: $\xi_0(z \approx 41\%)/a = 50(20)$ and $\nu_T(z \approx 41\%) = 0.72(7)$. A value of $\nu_T \approx 0.7$, together with $z_{S=1/2} = z_p$, is also obtained in a scaling analysis of our numerical data. We note that this value lies below $\nu_T = 0.90(5)$ for the $S = 5/2$ system $Rb_2(Mn,Mg)F_4$ [10]. Fits to the data at the highest concentration give $\nu_T = 0.70(7)$ and $\xi_0/a = 7(1)$.

The percolation threshold $z_p \approx 40.7\%$ is for the NN square lattice, and a non-zero frustrating next-NN (NNN) exchange could, in principle, shift z_p and lead to low-temperature spin-glass physics. The NNN exchange in La_2CuO_4 is expected to be frustrating and may be as large as $8\%J$ [18], which would lead to a small reduction of the ordered moment, but should not shift the critical point [10]. The dominant further-neighbor interaction may actually be a ring exchange among the four Cu sites on a square [29], which cannot extend connectivity beyond the NN

percolation threshold. In any case, further-neighbor interactions do not seem to noticeably affect the nature of the transition in $La_2Cu_{1-z}(Zn,Mg)_zO_4$, , $z_{S=1/2} = z_p$ within the uncertainty of our experiment, and we find no evidence of spin-glass behavior.

The correction terms to Eq. 1 can be expected to change as a result of the observed evolution of the low-temperature structure. Above $z \approx 25\%$, Néel order occurs in a low-temperature tetragonal phase. Nevertheless, we find that $T_N(z)$ evolves smoothly. Interestingly, our QMC data for Eq. 1 indicate that, as for undoped La_2CuO_4 [17], $T_N(z)$ corresponds very well to the temperature at which $\xi_{2D}/a = 100$, as shown in Fig. 2B. This suggests that any changes in the correction terms in the full spin Hamiltonian must be very subtle.

Assuming that quantum fluctuations do not alter the classical $T = 0$ correlation length exponent, $\nu_0 = \nu_{cl} = 4/3$ [8], our result of $\nu_T \approx 0.7$ suggests a crossover exponent $\Phi = \nu_0/\nu_T \approx 1.9$, which is larger than the values $\Phi = 1.43$ to 1.7 predicted theoretically [30, 31]. On the other hand, if $z = z_p$ is a quantum critical point, it would suggest a dynamical critical exponent of $z = 1/\nu_T \approx 1.4$. Series expansion and numerical approaches for the $S = 1/2$ bond percolation problem, which is closely related to the site percolation problem of the present study, predict $z = 1.7$ to 2 [32], whereas recent QMC work for the site-diluted $S = 1/2$ SLHAF arrives at $z \approx 2.5$ [14]. Our value is lower than these results, but also lies significantly above $z = 1$ for the Lorentz-invariant QNLσM [21], implying that the QNLσM fixed point is unstable to randomness.

Recent theoretical work for the randomly diluted $S = 1/2$ SLHAF has led to some exact results in the dilute limit of quantum impurities [1], and to interesting new predictions at higher concentrations [12, 16]. It has been argued that the presence of impurities should lead to localized spin excitations and to the breakdown of the classical hydrodynamic description of excitations in terms of spin waves above a characteristic length scale [16]. In this picture, the spin-wave velocity $c(z)$ is not a well-defined quantity, but there is no instability toward a disordered phase. Unlike dynamic observables, static properties such as the staggered magnetization and T_N remain well defined throughout the ordered phase. Because the spin-stiffness also remains well defined in this theory, one continues to expect the correlation length to have the low-temperature form $\xi \sim e^{2\pi\rho_s/T}$ as for the pure system. We have been able to determine $\xi(z,T)$ over a very wide range of impurity concentrations and temperature, and arrive at the unexpected conclusion that Eq. 2, and especially the heuristic crossover form Eq. 3, provide an excellent description of our data.

References

[1] S. Sachdev, C. Buragohain, M. Vojta, *Science* **286**, 2479 (1999).

[2] T. Matsuda, A. Fujioka, Y. Uchiyama, I. Tsukada, K. Uchinokura, *Phys. Rev. Lett.* **80**, 4566 (1998).

[3] M. Azuma, Y. Fujishiro, M. Takano, M. Nohara, H. Takagi, *Phys. Rev. B* **55**, 8658 (1997).

[4] M. Hücker, *et al.*, *Phys. Rev. B* **59**, R725 (1999).

[5] B. Keimer, *et al.*, *Phys. Rev. B* **46**, 14034 (1992).

[6] M. Corti, *et al.*, *Phys. Rev. B* **52**, 4226 (1995).

[7] K. Uchinokura, T. Ino, I. Terasaki, I. Tsukada, *Physica B* **205**, 234 (1995).

[8] D. Stauffer, A. Aharony, *Introduction to Percolation Theory, Revised* $2^{\rm nd}$ *Ed.* (Taylor and Francis, Bristol, PA, 1994).

[9] M. E. J. Newman, R. M. Ziff, *Phys. Rev. Lett.* **85**, 4104 (2000).

[10] R. J. Birgeneau, R. A. Cowley, G. Shirane, H. Yoshizawa, *J. Stat. Phys.* **34**, 817 (1984) and references therein.

[11] C. Yasuda, A. Oguchi, *J. Phys. Soc. Japan* **68**, 2773 (1999).

[12] Y.-C. Chen, A. H. Castro Neto, *Phys. Rev. B* **61**, R3772 (2000).

[13] S. Miyashita, J. Behre, S. Yamamoto, in *Computational Approaches in Condensed Matter Physics*, S. Miyashita, M. Imada, H. Takayama, Eds. (Springer, Berlin, 1992), pp. 97-111.

[14] K. Kato, *et al.*, *Phys. Rev. Lett.* **84**, 4204 (2000).

[15] A. W. Sandvik, preprint available at http://xxx.lanl.gov/abs/cond-mat/0110510.

[16] A. L. Chernyshev, Y. C. Chen, A. H. Castro Neto, preprint available at http://xxx.lanl.gov/abs/cond-mat/0107488.

[17] R. J. Birgeneau, *et al.*, *Phys. Rev. B* **59**, 13788 (1999).

[18] Y. J. Kim, *et al.*, *Phys. Rev. B* **64**, 4435 (2001).

[19] M. Greven, *et al.*, *Z. Phys. B* **96**, 465 (1995).

[20] B. B. Beard, R. J. Birgeneau, M. Greven, U.-J. Wiese, *Phys. Rev. Lett.* **80**, 1742 (1998).

[21] S. Chakravarty, B. I. Halperin, D. R. Nelson, *Phys. Rev. B* **39**, 2344 (1989).

[22] P. Hasenfratz, F. Niedermayer, *Phys. Lett. B* **268**, 231 (1991).

[23] A. Aharony, R. J. Birgeneau, A. Coniglio, M. A. Kastner, H. E. Stanley, *Phys. Rev. Lett.* **60**, 1330 (1988).

[24] K. Yamada, *et al.*, *Solid State Comm.* **64**, 753 (1987).

[25] M. Greven, R. J. Birgeneau, *Phys. Rev. Lett.* **81**, 1945 (1998).

[26] E. Manousakis, *Phys. Rev. B* **45**, 7570 (1992).

[27] A. H. Castro Neto, D. Hone, *Phys. Rev. Lett.* **76** (1996).

[28] A. B. Harris, S. Kirkpatrick, *Phys. Rev. B* **16**, 542 (1977).

[29] R. Coldea, *et al.*, *Phys. Rev. Lett.* **86**, 5377 (2001).

[30] H. E. Stanley, R. J. Birgeneau, P. J. Reynolds, J. F. Nicoll, *J. Phys. C* **9**, L553 (1976).

[31] A. Coniglio, *Phys. Rev. Lett.* **46**, 250 (1981).

[32] C. C. Wan, A. B. Harris, J. Adler, *J. Appl. Phys.* **69**, 5191 (1991).

33. O.P.V. and M.G. thank A. Aharony, A. H. Castro Neto, A. L. Chernyshev, A. W. Sandvik, and E. F. Shender for helpful discussions. The work at Stanford was supported by the U.S. Department of Energy under contract nos. DE-FG03-99ER45773 and DE-AC03-76SF00515, by NSF CAREER Award no. DMR9400372, and by the by the A.P. Sloan Foundation.

Table 1: Spin stiffness and spin-wave velocity extracted from fits of numerical data to Eq. 3. For $z < 35\%$, ν_T was fixed to be 1. At $z = 35\%$, a better fit was obtained using $\nu_T = 0.88(1)$. Equation 5 is modified by substitution of $1 + z$ for $1/P_\infty$, as discussed in the text. Theory for $c(z)$ is given by $c(z)/c(0) = A(z)(1 + z/2)$, as described in the text. The values for $2\pi\rho_s(0)$ and $c(0)$ are from [20].

z	$2\pi\rho_s(z)/J$	Modified Eq. 5	$c(z)/J/a$	Theory
0	1.18(1)	1.13	1.33(3)	1.66
0.08	0.79(1)	0.71	1.35(8)	1.31
0.20	0.31(1)	0.28	1.43(9)	0.79
0.31	0.063(1)	0.065	1.03(2)	0.34
0.35	0.026(1)	0.025	0.69(1)	0.18

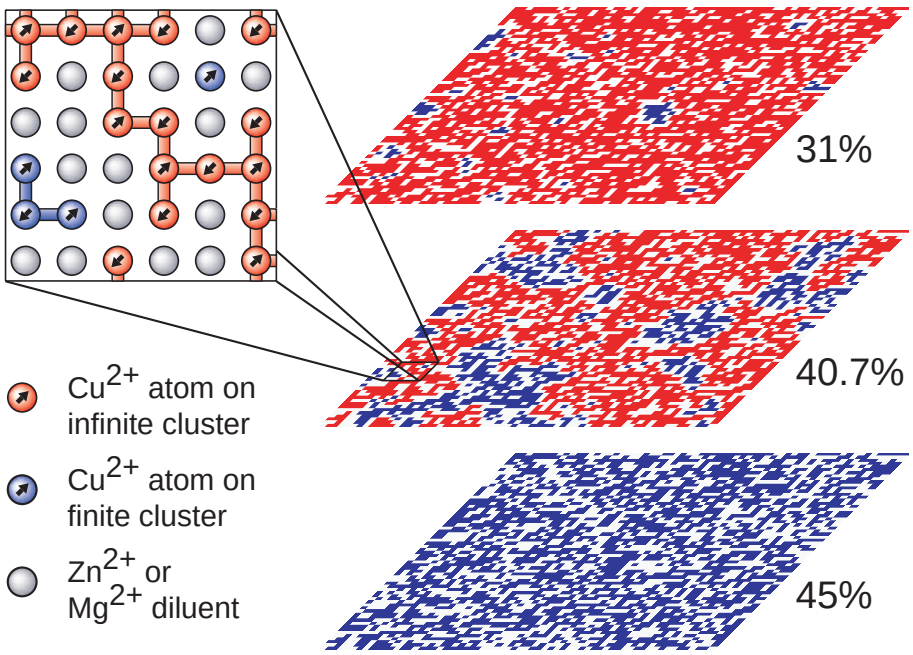

Figure 1: Schematic of finite-sized sections of the infinite square lattice with random site dilution levels well below (31%), just below (40.7%), and above (45%) the percolation threshold $z_p \approx 40.725\%$ [9]. Sites on the infinite cluster are shown in red, sites on finite disconnected clusters in blue, and diluents in white. The inset is a close-up view for $z = 40.7\%$, showing the role magnetic Cu and non-magnetic Zn/Mg ions play in the experimental system.

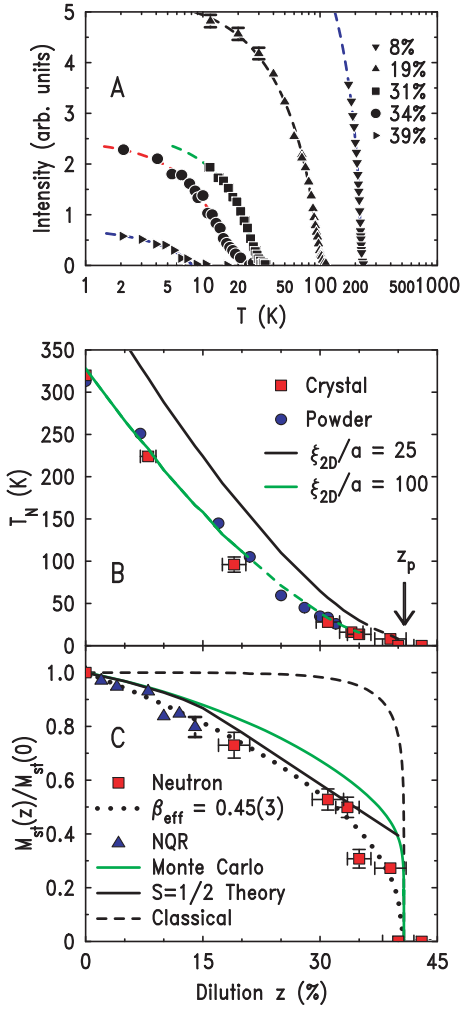

Figure 2: **(A)** (1,0,0) magnetic peak intensity from neutron diffraction (orthorhombic notation). A temperature-independent background has been subtracted. Lines represent fits for the magnetic order parameter squared, $\sim (T_N - T)^{2\beta}$ with $\beta \approx 0.30$, assuming a Gaussian distribution of T_N (typically $\approx$ 4 K) to describe the rounding due to the small inhomogeneities present in the large samples used. **(B)** T_N from neutron diffraction (crystal) and magnetometry (crystal and powder sample). Above $z \approx 20\%$, $T_N(z)$ deviates from an extrapolated line, approaching zero at the percolation threshold z_p. Lines correspond to constant correlation lengths ξ_{2D}/a = 25 and 100 from Monte Carlo simulations of the randomly diluted $S = 1/2$ NN SLHAF; dashed regions are extrapolated from higher temperature. **(C)** Staggered moment per Cu atom, normalized by the value for the pure system. The neutron data are consistent with previous NQR results [6]. The data are well described by a power law with $z_{S=1/2} = z_p$ and exponent $\beta_{eff} = 0.45(3)$. Also shown is recent QMC [15] and theory [16] for $S = 1/2$, as well as the classical ($S \to \infty$) result [15].

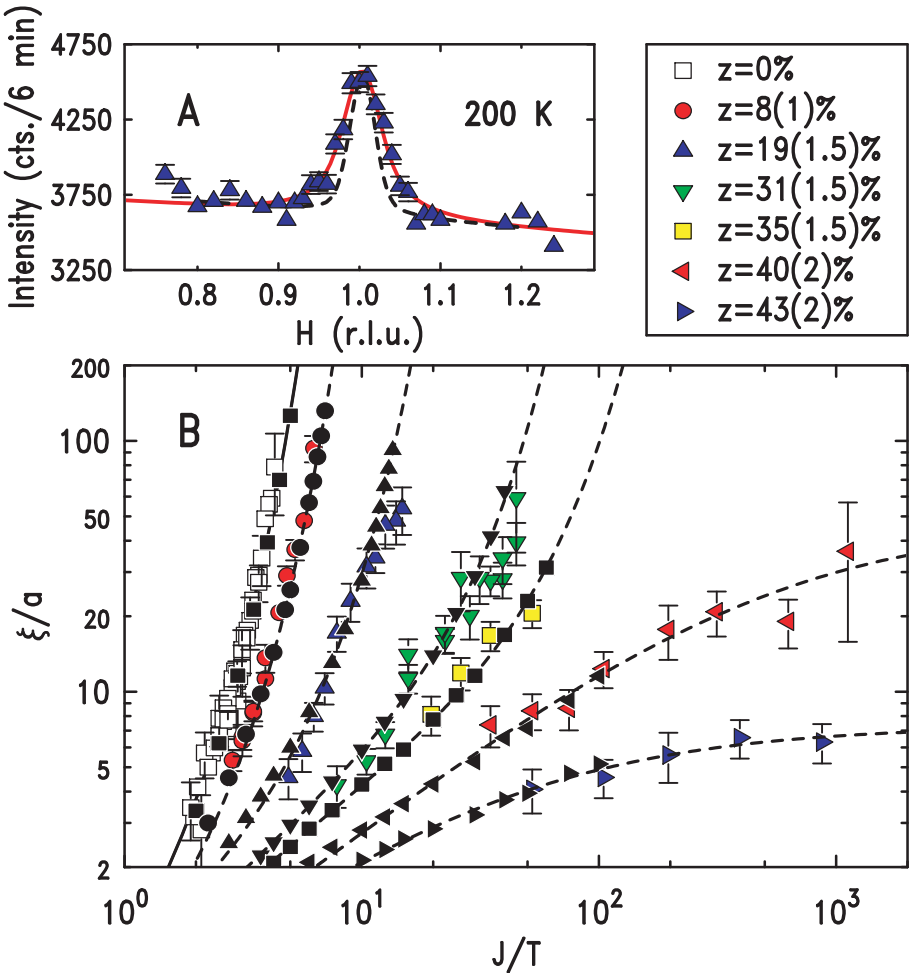

Figure 3: **(A)** Representative equal-time structure factor data. The solid red line represents a fit to the data, as discussed in the text, and the dashed black line indicates the instrumental resolution. This measurement was carried out in two-axis mode with 30.5 meV incident neutron energy and horizontal collimations of 40'-27.5'-sample-23.7'. **(B)** Spin-spin correlation lengths in units of the lattice constant. Colored symbols represent results from neutron scattering measurements of $La_2Cu_{1-z}(Zn,Mg)_zO_4$; black symbols represent Monte Carlo data for $z = 8, 20, 31, 35, 41$, and 46%. No adjustable parameters were used in the comparison. Experimental and numerical results for $z = 0$ are from [17, 20] and the solid line is Eq. 2. Dashed lines are fits to Eqs. 3 and 4, as discussed in the text.